

THE USE OF THERMOGRAPHY TO DETERMINE THE COMPACTION OF A SADDLE-SHAPED BRIQUETTE PRODUCED IN AN INNOVATIVE ROLLER PRESS COMPACTION UNIT

Michał BEMBENEK^{*}, Andrzej UHRYŃSKI^{**}

^{*}Department of Manufacturing Systems, Faculty of Mechanical Engineering and Robotics,
AGH University of Science and Technology, Al. Adama Mickiewicza 30, 30-059 Kraków, Poland

^{**}Department of Machine Design and Operation, Faculty of Mechanical Engineering and Robotics,
AGH University of Science and Technology, Al. Adama Mickiewicza 30, 30-059 Kraków, Poland

bembenek@agh.edu.pl, uhrynski@agh.edu.pl

received 25 June 2022, revised 11 September 2022, accepted 12 September 2022

Abstract: The unit compacting pressure in the fine-grained material consolidation process in the roller press can reach >100 MPa and is a parameter that results, among other things, from the properties of the consolidated material and the compaction unit geometry. Achieving the right pressure during briquetting is one of the factors that guarantee the proper consolidation and quality of briquettes. The distribution of the temperature on the surface of the briquettes correlates with locally exerted pressure. The present work aimed to analyse the briquetting process of four fine-grained materials in a roller press equipped with saddle-shaped briquette-forming rollers based on images obtained from the thermography conducted immediately after their consolidation. The tests were carried out in a roller press that was equipped with forming rollers of 450-mm diameter and having a cavity with a volume of 4 cm³, as described by patent PL 222229 B1. Two mixtures of hydrated lime with 9.1 wt% and 13.0 wt% water, a mixture of scale and a mixture of electric arc furnace (EAF) dust were used for the tests. In most mixtures, the highest temperatures were achieved in the middle-upper part of the briquettes. The briquettes from the EAF dust mixture heated locally the most on the surface up to 37.7 °C. The difference between the maximum briquette temperature and the ambient temperature was 20.2 °C.

Key words: roller press, thermography, thermovision, saddle-shaped briquettes, briquetting

1. INTRODUCTION

Many phenomena can be correlated with the temperature change of a tested object; therefore, it is important to obtain a precise picture of the distribution and increase of its surface temperature. The technique that makes it possible is thermography (it is based on measuring the radiation in the infrared range). Thermographic research finds increasingly wider possibilities of application, and it is used increasingly often; and this is a consequence, among other things, of the fact that the devices used for it allow for a set of steadily improving capabilities for measuring possibilities at lower costs of production and progressive miniaturisation. The decisive advantage of non-contact measurements is their non-invasiveness, which is often the basic criterion for selecting them.

Thermovision was originally used by the army to observe aeroplanes and detect the movement of military units. Until now, it has been successfully used for military purposes or the research related to, for example, the detection of defects in graphite nozzles used in missile propulsion systems [1] or to assess the technical condition of elements of military bridges [2]. Thermal imaging is widely used by the construction industry. It is useful for testing the energy efficiency of buildings, detecting defects in installation systems and verifying the effects of modernisation [3], as well as testing the thermal properties of walls [4], or detecting delamina-

tion of structural elements of buildings [5]. This technique, mainly due to its non-invasiveness, has been playing a special role in medicine for many years. It is used as a quick and precise tool to collect information necessary to diagnose rare diseases [6] or to evaluate the effectiveness of medical treatments [7]. It was also used to assess the impact of the body's reaction to low temperatures [8], vibrations [9] or workload [10].

However, it seems that the greatest spectrum of possibilities of using thermovision is provided by mechanical and electrical engineering. Thermography is very useful in the removal and treatment of material so as to control the increase and distribution of temperature in the tool working zone [11] and on the chip surface [12]. Its advantages were used in the assessment of welded joints and in the diagnosis of the course of the welding process itself [13, 14]. It should also be mentioned that this technique is used in the widely understood diagnostics of machines, ranging from numerically controlled machine tools [15], through rotating machines [16], belt conveyors [17], brakes [18] and rolling bearings (there is no way to measure the temperature of moving rolling elements and cage other than the contactless method) [19], up to electrical machines and devices [20, 21, 22]. The attempts to link strength and stress measurements in a material with the amount of heat energy produced are very interesting [23]. The methodology of measuring ropes has also been described, including the relation between temperature increase and stress increase in the

rope [24]. The relations between the mechanical properties of polypropylene stretching were analysed [25]; a system was suggested to analyse the thermomechanical properties and heat release in the stretching process [26]. Experiments have been carried out confirming the thesis that the analysis of temperature distribution in strength tests is the basis for the qualitative assessment of the stresses in the tested samples [27].

In addition to passive thermography (described above), we can also discuss active thermography, which is to be distinguished from the former variant in that it is a method of stimulating (arousing) the subject of research, e.g. by delivering an impulse in the form of thermal energy [28] or causing this effect by means of an acoustic wave [29], including ultrasounds [30] or microwaves [31], and then observing its path propagation and the effects that they have caused in the material using a thermograph on the surface of the tested object. This type of thermovision is particularly applicable in defectoscopy [32, 33].

Thermal phenomena are a rich source of information about technological processes and changes or irregularities taking place during these processes [34], which allows us to control the parameters of the process and to introduce the necessary modification so that the process runs properly and the product is of high quality. Thermography was used, among other purposes, for process control: casting and cooling of cast iron [35], production of casting moulds in order to form turbocharger blades [36], extrusion of poly (vinyl chloride) [37], production of tires [38] and the production of textiles [39, 40]. The quality of compacts made of loose materials leaving the compaction zone was also checked. Online monitoring of the powder flow during compaction helps to locate the areas of greatest pressure and identify the influence of the roller force on the powder temperature [41]. Recently, a study has been published that proposes a methodology to ascertain the extent to which the share material on the raking face undergoes wear during deployment in soil. The temperature distribution on the tool during operation was measured. Then, a hypothesis was made that the amount of heat emitted in a given area of the share surface correlates with the intensity of tribological processes [42].

An interesting issue is the use of thermography studies for agglomeration processes of fine-grained materials in a roller press [43]. During the production of a briquette in a roller briquetting press, the pressure exerted on its external surface is not uniform [44]. Depending on the place on the surface, it may have a variable value [45, 46]. The resulting compacting pressure distribution depends not only on the material properties but also on the geometry of the compaction unit and the briquette volume. The local compacting pressure exerted can be related to the temperature at the surface of the briquette. The higher the temperature at a given point in the briquette, the higher the compacting pressure exerted in this place. The results presented in this article are a continuation of previous research published in the literature that present a simultaneous study of the temperature distribution and the compacting pressures in various compacting units of the roller press. In previous works, the temperature distributions on the surface of classic saddle-shaped [47] and pillow-shaped briquettes [48] were presented. The tests presented in this article were carried out on four different mixtures of fine-grained materials in the innovative roller press compaction unit described by the PL 222229 B1 patent [49], in which the saddle-shaped cavities are distributed along the forming rollers. Compared with other compaction units, its geometry enables, among other utilities, self-synchronisation of working rollers, without the need for an additional gearbox.

2. MATERIALS AND METHODS

2.1. Briquetting process

The thermographic research of the briquetting process in the roller press was performed using a roller press (Fig. 1) with a 450-mm roller-pitch diameter with an installed PL 222229 B1 patented compaction unit for the production of pillow-shaped briquettes with dimensions of 31 mm × 24 mm × 11 mm and a rated capacity of 4 cm³ (Fig. 2). There were 30 forming cavities in each of the two rows on the surfaces of the forming rollers. The roller press was equipped with a 22-kW motor with a cycloidal gear and a frequency converter that enabled infinitely variable control of the rotation speed of the rollers. A gravity feeder was used when all materials were consolidated. The rollers' rotation speed was 0.85 RPM, which gave a peripheral speed of the rollers equal to 0.02 m/s. It caused each briquette in the forming row to fall out at approx. 2.0 s. The inter-roller gap was set to 1 mm.

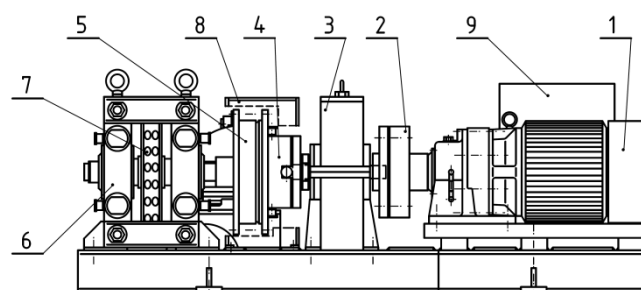


Fig. 1. The scheme of laboratory roller press (LPW 450): (1) gear motor with a cycloidal transmission, (2) flexible clutch, (3) gearbox, (4) Oldham clutch, (5) friction clutch, (6) moulding rollers cage, (7) forming rollers, (8) safety cover and (9) hydraulic system of sliding roller support

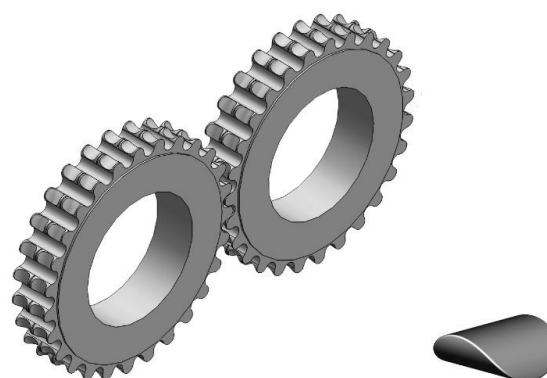


Fig. 2. The patented rollers PL 222229 B1 used in roller press compaction unit with a saddle-shaped briquette

Before the agglomeration process, four mixtures were prepared with the materials. They were thoroughly mixed in a Z-blade mixer with four rectangular mixing elements with dimensions of 190 mm × 90 mm and a shaft rotating speed of 55 RPM and brought to proper moisture, enabling them to be consolidated in a roller press, and the binders were added. The moisture content was determined using the weight method at 105 °C until a constant weight was obtained. The Vibra AJH 420 CE (Tokyo, Japan) scale was used.

2.2. Mixtures

2.2.1. Mixtures 1 (M1)

Its composition was 90.9 wt% calcium hydroxide manufactured by Lhoist (EN 459-1 CL 90-S) (Limelette, Belgium) and 9.1 wt% water. The average grain diameter was 19.9 μm. The mixture was mixed for about 30 min. The moisture content of the mixture was 9.4 wt%.

2.2.2. Mixture 2 (M2)

Its composition was 87.0 wt% calcium hydroxide manufactured by Lhoist (EN 459-1 CL 90-S) (Limelette, Belgium) and 13.0 wt% water. The average grain diameter was 19.9 μm. The mixture was mixed for about 30 min. The moisture content of the mixture was 13.2 wt%.

2.2.3. Mixture 3 (M3)

The mixture consisted of pre-compacted 92.6 wt% mill scale, with a grain size of ≤5 mm being obtained after the addition of water and molasses, each to an extent of 3.7 wt%. The mixture was mixed for about 10 min. Its moisture content was 5.2%. The pre-compacted process involved briquetting and crushing the consolidated briquettes to a size <10 mm.

2.2.4. Mixture 4 (M4)

The mixture contained 47.7 wt% of electric arc furnace dust (EAFD), 36.7 wt% of scale, 7.3 wt% fine coke breeze, 5.5 wt% 80° Bx molasses and 2.8 wt% calcium hydroxide. The last two ingredients were added as binders. The mixture was mixed for about 10 min. Its moisture content was 4.6%.

2.3. Thermography tests

The FLIR T1020 28° thermal imaging camera (Wilsonville, OR, USA) was used for the tests. The whole operating temperature range of the camera was from -40°C to +650°C, while the temperature range of -40°C to +150°C was used, for which the temperature measurement error was ±2°C or ±2% of the measurement value. The camera was equipped with a microbolometric matrix with a resolution of 1024 × 768 pixels, a 28° × 21° lens and a <0.0025 °C noise equivalent temperature difference (NETD) sensor. Before the tests, it was necessary to calibrate the camera. The ambient temperature during tests was 21.3 °C. The measuring station was prevented from having access to daylight and artificial light, since these were eliminated beforehand in the laboratory environment. In addition, a special shield was made (Fig. 3) to block the inflow of the light to the working area of the thermal imaging camera, and the purposes of this exercise were: (1) to eliminate the possibility of the reflection of radiation disturbing the test result and (2) to ensure repeatability of the distance measurement between the camera and the tested briquette.

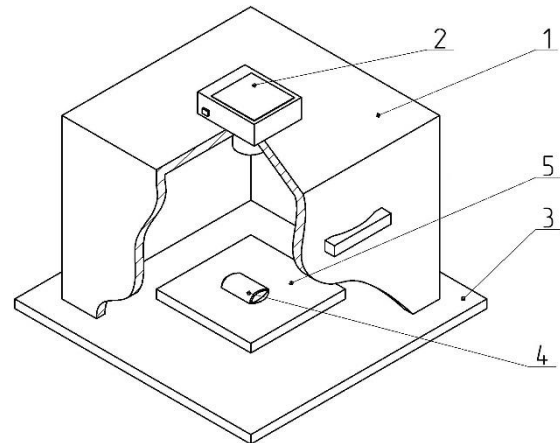


Fig. 3. A specially constructed station for capturing images of briquettes, which eliminates the effects of external radiation [48]: (1) cover; (2) thermal imaging camera; (3) base; (4) briquette; and (5) plywood pad

Each time the briquette was produced in a roller press, it was caught and transferred to a plywood plate, using heat-insulating gloves, immediately after leaving the compaction unit. Then, the briquettes and the pad were placed in a measuring station, and thermal images were captured. The time between catching the briquettes and capturing the photo was about 3 s. After each test, the plywood pad was changed to make the test conditions reproducible as the pads got hotter. The pads got hotter from the briquettes as time went on. It was possible to transfer the briquette to the plywood pad directly after it was removed from the compaction unit, while maintaining precise control of the briquette top-bottom, front-back orientation due to the low peripheral speed of the rollers (0.02 m/s). The tests of briquetting with the higher peripheral speed were unsuccessful due to the lack of possibility of controlled catching of the briquettes in the right orientation [47,48]. The images of the briquettes were captured in such a way that their 'top' (Fig. 4) was always located up the top edge of the image. Two briquettes were placed on the pads in two positions: 'front' and 'back', as shown in Fig. 4b.

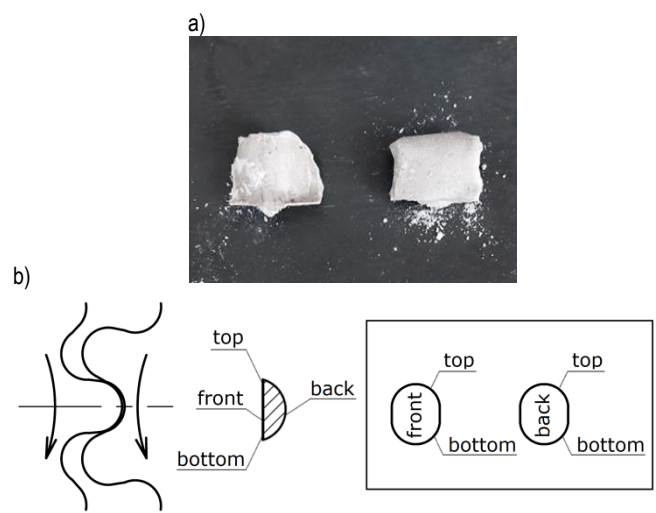


Fig. 4. The briquettes arrangement: (a) on the plywood pad (b) in the compacting unit

From each mixture, five thermal images of the briquettes were captured for further analysis. The FLIR Thermal Studio program (Wilsonville, OR, USA) was used to analyse the images. First, the maximum and minimum temperatures were determined for each type of briquette, and its measurements were averaged.

To examine the temperature distribution on the briquette surface, a special grid (shown in Fig. 5) was fitted into the thermograms. The measuring points were spaced 4.0 mm from each other. For each image in the vertical axis of the briquette at seven points, temperature values were read.

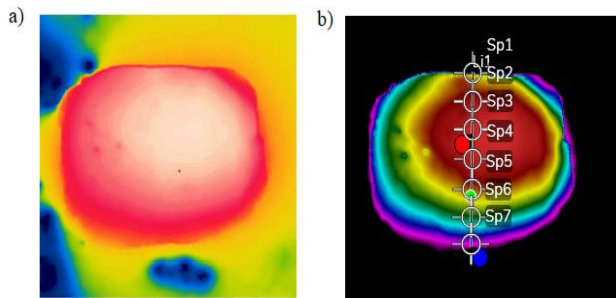


Fig. 5. Thermal image of the briquette: (a) thermal image from the camera, (b) thermal image processed in the FLIR Thermal Studio program with seven temperature measurement points superimposed

The emissivity of the integrated materials was determined according to previously developed procedures [48] with the use of the FLIR Thermal Studio program. Pilot batches of briquettes, from each of the mixtures, were prepared. The briquettes were then seasoned at ambient temperature for 24 h. Then, briquettes were deposited in a SPT-200 furnace (ZUT Colector, Kraków, Poland), which had been previously heated to 59 °C for 20 min to ensure that the temperature prevailing in them would be higher than the ambient temperature. The temperature of the furnace was measured using a Kyoritsu KEW 1011 multimeter and K-type 8216 thermocouple (Kyoritsu, Tokyo, Japan). After removing the briquettes from the furnace, their thermal images were captured and processed in the FLIR Thermal Studio program.

3. RESULTS AND DISCUSSION

From all the materials used in the tests, high-quality briquettes that did not crumble were obtained.

3.1. Emissivity

The emissivity results of individual materials are presented in Tab. 1. All tested materials showed high emissivity, which is a desirable feature. This allows us to perform thermographic measurements with minimal measurement errors. Mixture M2 showed the highest emissivity. The difference between the highest and the lowest emissivity is 0.17. The above cases of emissivity were taken into account appropriately for each type of briquette in the images analysed.

Tab. 1. Emissivity of briquettes

Mixture	Emissivity, $\epsilon -$
M1	0.81
M2	0.98
M3	0.86
M4	0.85

3.2. Differences in temperature on the surface of briquettes

The results of the minimum and maximum temperature for each type of briquette on the front and back sides are presented in Fig. 6. The research showed that the temperature on the surface of the briquettes differed depending on the mixture used for consolidation.

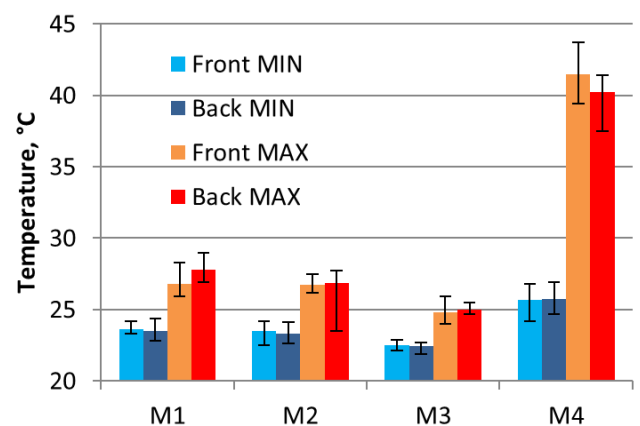


Fig. 6. The graphs of average minimum and maximum temperature measurements on the surface

The highest temperature on the whole surface of the briquettes was obtained for mixture M4 (EAFD mixture). It amounted to 41.5 °C and was 20.2 °C higher than the ambient temperature. The lowest maximum temperature was obtained for mixture M3. The difference in maximum temperatures between the materials was 16.5 °C. The lowest minimum temperature was obtained for mixture M3. It was still higher than the ambient temperature by 1.1 °C. In this case, a relatively low unit compacting pressure during compaction can be expected.

3.3. Temperature distribution on briquette surfaces

The results of the temperature distribution on the briquette front surfaces for each type of briquette are presented in Fig. 7. As in the case of other compaction units, the temperature on the surface of the briquettes turned out to be non-uniform. The highest temperature is obtained in the upper middle part of the briquette. In this part of the briquette from the front side, one can therefore expect the greatest packing of the material, resulting from the greatest compacting pressure acting at this point [46]. These results coincide with the simulation tests carried out for briquetting of fine-grained materials using the discrete element method [50]. The temperature distribution curve for material M4 differs from the other curves. In point 2, the temperature is not higher than in point 1, which is the case with other curves. It can

be assumed that the volume of the moulding cavities used for this mixture is too small. The mixture is overpressed, the structure of the briquettes is destroyed and defects appear in the briquettes. This can be seen in Fig. 8.

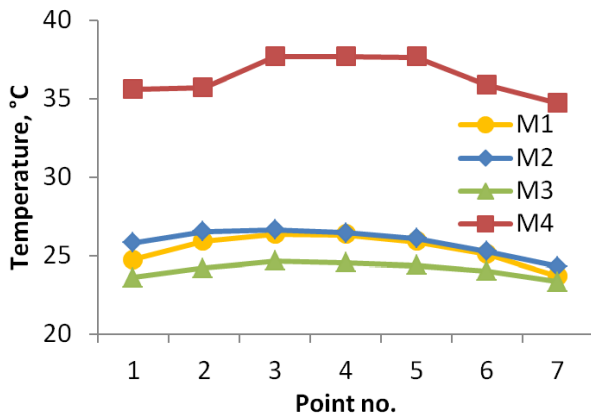


Fig. 7. The temperature distribution on the front side of the briquette surfaces

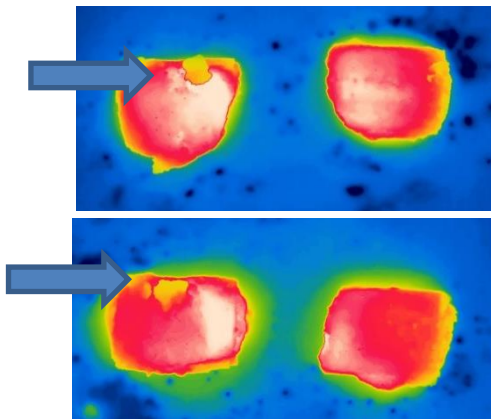


Fig. 8. Thermographic image with the damaged structure of the briquette from M4 mixture

The results of the temperature distribution on the briquette back surfaces are presented in Fig. 9.

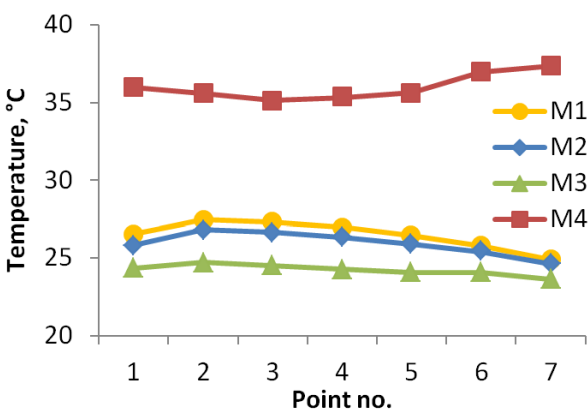


Fig. 9. The temperature distribution on the back side of briquette surfaces

For M1, M2 and M3 mixtures, the highest temperature on the back side of the briquette was obtained in point 2. The tempera-

ture distribution for these materials takes the form of a parabola directed downwards. This means that the minimum temperatures are at the top and bottom of the briquette. The M4 material, in turn, has the highest recorded temperatures in the upper and lower parts of the briquette, differently for the remaining mixtures. This is probably owing to the volume of the cavity being too small for this type of mixture, and its overpressing is caused by the exertion of excessive pressure on the material, which was also noticed on the front side of the briquette. No defects were noticed on this side of the briquettes. The difference in the temperature distribution between the M1 and M2 mixes, i.e. mixes with the same composition but with different moisture content, proved that the moisture had an influence on the unit pressure during briquette formation [51].

4. CONCLUSION

The conducted research proved that thermographic methods can be indirectly used to describe the phenomena occurring in the roller press compacting unit as described by the patent PL 222229 B1. As experience shows, the method requires special preparation of the test stand to eliminate the influence of undesirable external factors, such as radiation sources, that may prevent the reliable processing of the obtained results.

For M1, M2 and M3 mixtures, similar results of temperature distributions were obtained as in the case of the classic compaction system for the production of saddle-shaped and pillow-shaped briquettes. The highest obtained temperature was obtained in the middle-upper part of the briquette. For the EAFD mixture, the temperature distribution curves turned out to be different. This is probably due to the volume of the forming cavities being too small for this type of material. Additionally, thermographic tests showed defects in briquettes made of M4 mixture. This confirms the hypothesis that thermography as an indirect method can be used to test the correctness of the selection of the type of the roller press compaction unit and the volume of briquettes.

In the authors' opinion, the tests are utilitarian, as they show the possibility of using thermographic tests to assess the quality of briquettes in industrial conditions.

Further research is planned to determine the correlation between the local temperature of the material and the compacting pressure exerted there. A special stand has been developed for this purpose.

REFERENCES

- Świdorski W, Miszczak M, Szabra D. Zastosowanie pomiarów termowizyjnych w badaniach dysz grafitowych stosowanych układach napędowych przeciwlotniczych pocisków raketowych krótkiego zasięgu. *Biuletyn Wojskowej Akademii Technicznej*. 2008;57(3): 285-293.
- Duchaczek A, Mańko Z. Próba zastosowania termowizji w badaniach zmęczeniowych dźwigarów stalowych w mostach wojskowych. *Zeszyty Naukowe / Wyższa Szkoła Oficerska Wojsk Łądowych im. gen. T. Kościuszki*. 2009;(3): 125-135.
- Al-Habaibeh A, Hawas A, Hamadeh L, Medjdoub B, Marsh J, Sen A. Enhancing the sustainability and energy conservation in heritage buildings: The case of Nottingham Playhouse. *Frontiers of Architectural Research*. 2022;11(1): 142-160. <https://doi.org/10.1016/j.foar.2021.09.001>

4. Silva GP, Batista PIB, Povóas YV. The usage of infrared thermography to study thermal performance of walls: a bibliographic review. *Revista ALCONPAT*. 2019;9(2): 117-129. <https://doi.org/10.21041/ra.v9i2.341>
5. Tomita K, Chew MYL. A Review of Infrared Thermography for Delamination Detection on Infrastructures and Buildings. *Sensors*. 2022;22(2): 423. <https://doi.org/10.3390/s22020423>
6. Branco JHL, Branco RLL, Siqueira TC, de Souza LC, Dalago KMS, Andrade A. Clinical applicability of infrared thermography in rheumatic diseases: A systematic review. *Journal of Thermal Biology*, 2022, 104, 103172 <https://doi.org/10.1016/j.jtherbio.2021.103172>
7. Kaźmińska B, Sobiech KA, Demczuk-Włodarczyk E, Chwałczyńska A. Thermovision assessment of temperature changes in selected body areas after short-wave diathermy treatment. *Journal of Thermal Analysis and Calorimetry*. 2021: 1-8 <https://doi.org/10.1007/s10973-021-11136-z>
8. Damijan Z, Uhryński A. Systemic cryotherapy influence of low temperatures on selected physiological parameters. *Acta Physica Polonica A* 2012;121(1-A): 38-41. <http://dx.doi.org/10.12693/APhysPolA.121.A-38>
9. Damijan Z, Uhryński A. The effect of general low frequency vibration on energy balance of a human being. *Acta Physica Polonica A*. 2013;123(6): 970-973. doi: 10.12693/APhysPolA.123.970
10. Damijan Z, Uhryński A. The influence of driver's working environment on thermal changes of their organism. *Acta Physica Polonica A*. 2010;118(1): 35-40. doi: 10.12693/APhysPolA.118.35
11. Molenda J, Charchalis A. Using thermovision for temperature measurements during turning process. *Journal of KONES Powertrain and Transport*. 2018;25(4): 293-298. <https://doi.org/10.5604/01.3001.0012.4803>
12. Bartoszek M. Thermovision measurements of temperature on the tool-chip upper side in turning of aisi 321 steel. *Technical Sciences*. 2020;23(1): 69-80. <https://doi.org/10.31648/ts.5177>
13. Piecuch G, Madera M, Żabiński T. Diagnostics of welding process based on thermovision images using convolutional neural network. *IOP Conf. Series: Materials Science and Engineering*. 2019;710(1): 012042. doi: 10.1088/1757-899X/710/1/012042
14. Nowacki J, Wypych A. Application of thermovision method to welding thermal cycle analysis. *The Journal of Achievements in Materials and Manufacturing Engineering*. 2010;40(2): 131-137.
15. Struzikiewicz G, Sioma A. Application of infrared and high-speed cameras in diagnostics of CNC milling machines: case study. *Photonics Applications in Astronomy, Communications, Industry, and High-Energy Physics Experiments*. 2019;11176: 111760c. <https://doi.org/10.1117/12.2536679>
16. Fidal M. Identification of machine technical state on the basis of fourier analysis of infrared images. *Diagnostics And Structural Health Monitoring*. 2011;2(58): 25-30.
17. Michalik P, Zajac J. Use of thermovision for monitoring temperature conveyor belt of pipe conveyor. *Applied Mechanics and Materials*. 2014;683: 238-42. <https://doi.org/10.4028/www.scientific.net/AMM.683.238>
18. Baranowski P, Damaziak K, Malachowski J, Mazurkiewicz L, Polakowski H, Piatkowski T, Kastek M. Thermovision in the validation process of numerical simulation of braking. *Metrology and Measurement Systems*. 2014;21(2): 329-340. <http://dx.doi.org/10.2478/%2Fmms-2014-0028>
19. Jakubek B, Grochalski K, Rukat W, Sokol H. Thermovision measurements of rolling bearings. *Measurement*. 2022;189: 110512. <https://doi.org/10.1016/j.measurement.2021.110512>
20. Janura R, Gutten M, Korenciak D, Sebok M. Thermal processes in materials of oil transformers. *Dagnostic of Electrical Machines and Insulating Systems in Electrical Engineering (DEMISEE)*. 2016: 81-84. doi: 10.1109/DEMISEE.2016.7530470
21. Simko M, Chupac M, Gutten M. Thermovision measurements on electric machines. *International Conference on Diagnostics in Electrical Engineering (Diagnostika)*. 2018: 1-4. doi: 10.1109/DIAGNOSTIKA.2018.8526033
22. Wyleciał T, Urbaniak D. Research on thermal contact resistance in a bed of steel square bars using thermovision. *Acta Physica Polonica A*. 2019;135(2): 263-269. doi: 10.12693/APhysPolA.135.263
23. Sharkeev Y, Vavilov V, Skripnyak V.A, Belyavskaya O, Legostaeva E, Kozulin A, Chulkov A, Sorokoletov A, Skripnyak VV, Eroshenko A, Kuimova M. Analyzing the deformation and fracture of bioinert titanium, zirconium and niobium alloys in different structural states by the use of infrared thermography. *Metals*. 2018; 8(9): 703. <https://doi.org/10.3390/met8090703>
24. Heinz D, Halek B, Krešák J, Peterka P, Fedorko G Molnár V. Methodology of measurement of steel ropes by infrared technology. *Engineering Failure Analysis*. 2022;133: 105978. <https://doi.org/10.1016/j.engfailanal.2021.105978>
25. Pawlak A, Rozanski A, Galeski A. Thermovision studies of plastic deformation and cavitation in polypropylene. *Mechanics of Materials*. 2013;67: 104-118. <https://doi.org/10.1016/j.mechmat.2013.07.016>
26. Košťál P, Ružiak I, Jonšta Z, Kopal I, Hrehuš R, Kršková J. Experimental method for complex thermo-mechanical material analysis. *International Journal of Thermophysics*. 2010;31: 630-636. <https://doi.org/10.1007/s10765-010-0745-5>
27. Piekłak K, Mikołajczyk Z. Strength tests of 3D warp-knitted composites with the use of the thermovision technique. *Fibres & Textiles in Eastern Europe*. 2011;19(5 (88)): 100-105.
28. Grochalski K, Peta K. Diagnostic methods of detecting defects within the material with the use of active infrared thermovision. *Archives of Mechanical Technology and Materials*. 2017;37(1): 41-44. doi: 10.1515/amtm-2017-0006
29. Bazaleev NI, Bryukhovetskij VV, Klepikov VF, Litvinenko VV. Thermovision acoustic thermography construction materials defectoscopy. *Voprosy Atomnoj Nauki i Tekhniki. Fizika Radiatsionnykh Povrezhdenij i Radiatsionnoe Materialovedenie*. 2011;2(97/72): 178-185.
30. Wierzbicki Ł, Stabik J, Wróbel G, Szczepanik M. Efficiency of two non-destructive testing methods to detect defects in polymeric materials. *Journal of Achievements in Materials and Manufacturing Engineering* 2010;38(2): 163-170.
31. Durka T, Stefanidis G, Van Gerven T, Stankiewicz A, On the accuracy and reproducibility of fiber optic (FO) and infrared (IR) temperature measurements of solid materials in microwave applications. *Measurement Science and Technology*. 2010;21(4): 045108. <http://dx.doi.org/10.1088/0957-0233/21/4/045108>
32. Lahiri BB, Bagavathiappan S, Reshmi PR, Philip J, Jayakumar T, Raj B. Quantification of defects in composites and rubber materials using active thermography. *Infrared Physics & Technology*. 2012;55(2-3): 191-199. <https://doi.org/10.1016/j.infrared.2012.01.001>
33. Rózański L, Ziopaja K. Detection of material defects in reinforced concrete slab using active thermography. *Measurement Automation Monitoring*. 2017;63(3): 82-85.
34. Miękina W, Madura H. Podstawy teoretyczne pomiarów termowizyjnych. *Pomiary termowizyjne w praktyce. Agenda Wydawnicza Paku*. 2004: 10-26.
35. Lepiarczyk D, Uhryński A. Thermo-Vision Analysis of Iron Foundry Production Process Concerning Secondary Usage of Heat. *Polish Journal of Environmental Studies*. 2014;23(3): 1017-1023.
36. Żaba K, Nowak S, Kwiatkowski M, Nowosielski M, Kita P, Sioma A. Application of non-destructive methods to quality assessment of pattern assembly and ceramic mould in the investment casting elements of aircraft engines. *Archives of Metallurgy and Materials*. 2014;59(4): 1517-1525. doi: 10.2478/amm-2014-0250
37. Tor-Świątek A, Samuń B. Use of thermo vision research to analyze the thermal stability of microcellular extrusion process of poly(vinyl chloride). *Maintenance and Reliability*. 2013;15(1): 58-61.
38. Hynek M, Votapek P. Thermal analysis of tyre curing process. *Engineering mechanics, 17th international conference. Prague*. 2011: 223-226.
39. Kašiković N, Novaković D, Milić N, Vladić G, Zeljković Ž, Stančić M. Thermovision and spectrophotometric analysis of ink volume and material characteristics influence on colour changes of heat treated printed substrates. *Technical Gazette*. 2015;(22)1: 33-41. doi: 10.17559/TV-20130928115500
40. Michalak M. Non-contact tests of thermal properties of textiles, Part 1. (Bezkontaktowe badania właściwości cieplnych wyrobów włókienniczych. Cz. 1.) *Przegląd Włókienniczy - Włókno, Odzież, Skóra*. 2010; 2: 31-33.

41. Litstera JD, Omara C, Salman AD, Yua M, Weidemann M, Schmidt A. Roller compaction: Infrared thermography as a PAT for monitoring powder flow from feeding to compaction zone. *International Journal of Pharmaceutics*. 2020;578: 119114. <https://doi.org/10.1016/j.ijpharm.2020.119114>
42. Kostencki P, Stawicki T, Króllicka A. Wear of Ploughshare Material With Regards to the Temperature Distribution on the Rake Face When Used in Soil. *Journal of Tribology*. 2022;144(4): 041704. <https://doi.org/10.1115/1.4053586>
43. Yu M, Omar C, Weidemann M, Schmidt A, Litster JD, Salman AD. Roller compaction: Infrared thermography as a PAT for monitoring powder flow from feeding to compaction zone. *Int J Pharm* [Internet]. 2020;578(119114):119114. Available from: <https://www.science-direct.com/science/article/pii/S0378517320300983>
44. Bembenek M, Krawczyk J, Pańcikiewicz K. The wear on roller press rollers made of 20Cr4/1.7027 steel under conditions of copper concentrate briquetting. *Materials (Basel)* [Internet]. 2020 [cited 2022 Jun 14];13(24):5782. Available from: <https://www.mdpi.com/1996-1944/13/24/5782>
45. Bembenek M. Exploring efficiencies: Examining the possibility of decreasing the size of the briquettes used as the batch in the electric arc furnace dust processing line. *Sustainability* [Internet]. 2020 [cited 2022 Jun 14];12(16):6393. Available from: <https://www.mdpi.com/2071-1050/12/16/6393>
46. Bembenek M, Krawczyk J, Frocisz Ł, Śleboda T. The analysis of the morphology of the saddle-shaped bronze chips briquettes produced in the roller press. *Materials (Basel)* [Internet]. 2021 [cited 2022 Jun 14];14(6):1455. Available from: <https://www.mdpi.com/1996-1944/14/6/1455>
47. Bembenek M, Uhryński A. Analysis of the temperature distribution on the surface of saddle-shaped briquettes consolidated in the roller press. *Materials (Basel)* [Internet]. 2021 [cited 2022 Jun 14];14(7):1770. Available from: <https://www.mdpi.com/1996-1944/14/7/1770>
48. Uhryński A, Bembenek M. The thermographic analysis of the agglomeration process in the roller press of pillow-shaped briquettes. *Materials (Basel)* [Internet]. 2022 [cited 2022 Jun 14];15(8):2870. Available from: <https://www.mdpi.com/1996-1944/15/8/2870>
49. Hryniewicz M., Janewicz A. Briquetting device. Polish patent, PL 222229 B1, July 29, 2016
50. Bembenek M, Buczak M, Baiul K. Modelling of the Fine-Grained Materials Briquetting Process in a Roller Press with the Discrete Element Method. *Materials*. 2022; 15(14):4901. <https://doi.org/10.3390/ma15144901>
51. Bembenek M. Exploring Efficiencies: Examining the Possibility of Decreasing the Size of the Briquettes Used as the Batch in the Electric Arc Furnace Dust Processing Line. *Sustainability*. 2020; 12(16):6393. <https://doi.org/10.3390/su12166393>

We would like to thank Mr. Gabriel Grzebinoga for his help during the research.

Michał Bembenek:  <https://orcid.org/0000-0002-7665-8058>

Andrzej Uhryński:  <https://orcid.org/0000-0001-8832-7873>